Available online at www.sciencedirect.com
ScienceDirect
Catalysis Communications 9 (2008) 1432–1438
CATALYSIS COMMUNICATIONS
www.elsevier.com/locate/catcom

Synthesis of a supported nickel boride catalyst under microwave irradiation

Zhi-Jie Wu, Shao-Hui Ge, Ming-Hui Zhang *, Wei Li, Ke-Yi Tao

Institute of New Catalytic Materials Science, College of Chemistry and Engineering Research Center of High-Energy Storage & Conversion (Ministry of Education), Nankai University, Tianjin 300071, PR China

Received 28 June 2007; received in revised form 6 December 2007; accepted 9 December 2007
Available online 23 December 2007

Abstract

Supported nickel boride (Ni–B) catalysts were prepared by a silver-catalyzed electroless plating method under microwave irradiation. Two solvents of plating solution, water and ethylene glycol, were used to study the effect of microwave irradiation on plating. The Ni–B catalysts were characterized by X-ray diffraction, transmission electron microscopy, and X-ray photoelectron spectroscopy. Their catalytic performances were evaluated by hydrogenation of acetophenone. The results showed that the particle size and load of Ni–B increased much more under microwave irradiation, when the water was used as solvent. The supported Ni–B catalyst prepared from ethylene glycol bath exhibited higher catalytic activity and selectivity in the hydrogenation, due to its higher boron content in Ni–B particles.

Keywords: Microwave irradiation; Nickel boride; Electroless plating; Hydrogenation

1. Introduction

Metal boride catalyst has attracted much attention over the past 50 years, due to its refractory nature, resistance to sulfur poisoning, desulphurization ability in organic synthesis, and catalytic properties [1,2]. Among various metal borides, nickel boride (Ni–B) is regarded as a potential industrial catalyst for hydrogenation reactions [3,4]. Ni–B nanoparticles are deposited on various supports to prepare supported catalysts, which exhibit better thermal stability and catalytic activities [5]. The supported Ni–B catalyst is usually synthesized by an impregnation-reduction method [4,5]. However, such method is difficult to carry out in industrial preparation [4]. Chen et al. synthesized a Ni–B catalyst by an electroless plating method, and found it showed superior catalytic property to the corresponding Ni–B catalyst prepared by a chemical reduction method [6]. It suggests that the electroless plating method is a promising route to synthesize active Ni–B catalysts. We also have found that supported Ni–B catalysts can be prepared by a silver-catalyzed electroless plating method [7–11]. In this work, we prepared the supported Ni–B catalyst under microwave irradiation to change the properties of Ni–B particle, such as its morphology and particle size.

Microwave irradiation as a heating method has been found a number of applications in chemistry since 1986 [12,13]. The effect of heating is generated by the interaction of a dipole moment of the molecules with high frequency electromagnetic radiation. Unlike conventional heating, microwave irradiation is characteristic in its selective, local heating [14]. Conner et al. studied the effect of microwave irradiation on the sorption of oxides [14–18]. They found that the temperature at the surface where sorption occurs was "effectively" greater than the measured solid or gas temperature, since oxides had a low permittivity and were relatively transparent to microwave during the sorption on oxide solids [17]. As different adsorbates had different capabilities to adsorb microwave energy, different local temperatures and sorption selectivities on oxides solids

* Corresponding author. Tel./fax: +86 22 23507730.
E-mail address: zhangmh@nankai.edu.cn (M.-H. Zhang).

1566-7367/$ - see front matter © 2007 Elsevier B.V. All rights reserved.
doi:10.1016/j.catcom.2007.12.006

occurred under microwave irradiation [15]. It means that the adsorbates are adsorbed selectively on the oxides under microwave irradiation. Consequently, this principle can be extended to prepare oxides supported catalysts, in order to control the selective deposition of active metal on supports. For studying the effect of microwave irradiation on the deposition of Ni–B particles, water and ethylene glycol (EG) with different permittivity were selected as solvents for experiments. The resulting catalysts were characterized by X-ray diffraction (XRD), transmission electron microscopy (TEM), and X-ray photoelectron spectroscopy (XPS). The catalytic performances of catalysts were evaluated by a selective hydrogenation of acetophenone (AP).

2. Experiment section

2.1. Catalyst preparation

Ag/MgO was synthesized as Ref. [7]. 0.02 g $AgNO_3$, 0.15 g ammonia, 0.005 g NaOH, and 0.002 g HCHO were dissolved in 425 distilled water. Then, some MgO was added to the solution and stirred at 313 K for 4 h. The resulting Ag/MgO was washed with water and dried at 363 K for 4 h. The Ag loading was controlled at 0.2 wt%. Deposition of Ni–B on the Ag/MgO support was performed by adding the support to a basic borohydride bath of the following compositions: $NiSO_4 \cdot 6H_2O$, 12.0 g/L; KBH_4, 5.5 g/L; ethylenediamine (en), 10.0 g/L; and NaOH, amount needed to maintain the desirable pH value (ca. 13.4–13.5). The plating was carried out by conventional heating or microwave irradiation (2455 MHz) at 323 K. It lasted until no significant bubbles were observed. The product was washed with water thoroughly to get a pH value of 7, then washed with ethanol for several times and stored in ethanol. The theoretic nickel loading was controlled between 15 and 20 wt%. The microwave irradiation power was selected between 0 and 180 W. The solvent of plating solution was water or ethylene glycol (EG), and the resulting Ni–B/MgO catalysts were denoted as Ni–B/MgO(W) and Ni–B/MgO(EG), respectively.

2.2. Catalyst characterization

XRD patterns of the samples were acquired on a Rigaku D/max-2500 powder diffractometer employing Cu Kα source ($\lambda = 1.5418$ Å). The chemical compositions of the samples were analyzed by inductively coupled plasma atomic emission spectrometry (ICP-AES) on an IRIS Intrepid spectrometer. TEM images of catalysts were acquired using a JEOL-2010 FEF high resolution transmission electron microscope. XPS was carried out with a Kratos Axis Ultra DLD spectrometer employing a monochromated Al Kα X-ray source, hybrid (magnetic/electrostatic) optics and a multi-channel plate and delay line detector (DLD). To avoid the influence of the surface oxygen, argon etching for 10 min was performed to remove the surface oxide layer.

2.3. Catalyst testing

The catalytic experiments were carried out in a 100 ml stainless steel autoclave. The stirring effect was preliminarily investigated and a stirring rate of 800 rpm was employed, which turned out to be sufficient to eliminate the diffusion limit. In the hydrogenation of AP, 0.6 g dry catalyst (dried in 100 ml/min N_2 flow), 5.0 g (42.8 mmol) AP and 60.0 ml ethanol were mixed. The reaction was carried out at 373 K for 1 h. The H_2 pressure was 1.0 MPa. The hydrogenation product was analyzed by a gas chromatograph equipped with a flame ionization detector.

3. Results and discussion

For the silver-catalyzed electroless plating [7], the plating is activated by the silver clusters preloaded on the supports, and the Ni–B clusters are formed and distributed selectively on the defective sites of supports, such as edges, pores, or corners [19,20], which result in new active sites for Ni–B deposition. The plating is driven by an autocatalysis effect of the resulting Ni–B clusters after silver catalyzing, then all the Ni–B clusters deposit selectively on the active surface of supports. In short, the dispersion and properties of Ni–B particles are mainly depended on the interaction between surface of support and plating solution (Stern–Grahame electrical double layer) [21]. In other words, the properties of Ni–B can be modified by changing supports or solvents to affect the sorption of supports. In this paper, two solvents, water and EG, were used to study the sorption of MgO under microwave irradiation according to work of Conner et al. [14–18].

3.1. Synthesis of supported Ni–B catalyst

Fig. 1 shows the TEM micrographs of supported Ni–B/MgO(W) and Ni–B/MgO(EG) prepared by conventional heating. The Ni–B particles are distributed homogeneously over MgO. The particles size of Ni–B is ~45 nm for Ni–B/MgO(EG) and ~40 nm for Ni–B/MgO(W). The compositions of both samples are listed in Table 1. The content of boron in Ni–B/MgO(EG) is higher than that in Ni–B/MgO(W), suggesting that the deposition process of nickel and boron is affected by the solvent. Table 1 also shows the compositions of supported Ni–B prepared in different solvents with different microwave irradiation powers. For Ni–B/MgO(W) samples, the composition of Ni–B is almost identical without the influence of irradiation power. The nickel content of Ni–B particles in Ni–B/MgO(EG) decreases when microwave irradiation is applied. The Ni loading on Ni–B/MgO(W) and Ni–B/MgO(EG) catalysts increases under microwave irradiation, especially when a lower irradiation power is used. The increase of Ni loading may be ascribed to two factors: (1) the interaction between the active sites for deposition of Ni–B and adsorbates was affected by the microwave irradiation. For instant, it may change the oxidation potential of the borohydride to be less

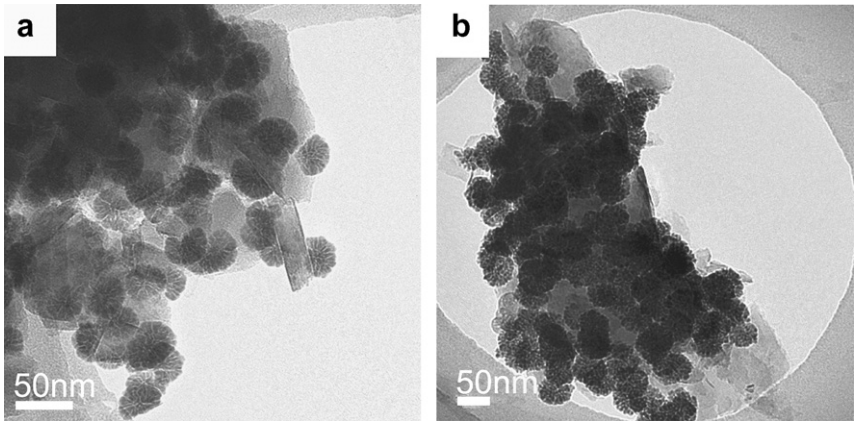

Fig. 1. TEM micrographs of supported Ni–B/MgO samples prepared from (a) water bath, and (b) EG bath.

Table 1
The compositions of Ni–B/MgO samples

Samples	Power of microwave (W)	Load of Ni (wt%)	Compositions (at%)
Ni–B/MgO(W)	0	10.7	$Ni_{75.5}B_{24.5}$
Ni–B/MgO(W)	120	11.0	$Ni_{75.8}B_{24.2}$
Ni–B/MgO(W)	60	11.9	$Ni_{76.1}B_{23.9}$
Ni–B/MgO(EG)	0	10.5	$Ni_{69.3}B_{30.7}$
Ni–B/MgO(EG)	120	10.8	$Ni_{65.4}B_{34.6}$
Ni–B/MgO(EG)	60	11.2	$Ni_{61.8}B_{38.2}$

noble to the reversible potential of the metal [22]. (2) The equilibrium of the plating solution was changed by microwave irradiation. The heating effect of microwave irradiation was generated by the interaction of the dipole moment of the molecules with the high frequency electromagnetic radiation. On the other hand, the lower power of microwave irradiation results in a higher Ni loading (Table 1). It can be explained as follows: The oxide sorption under microwave irradiation was mainly depended on the time, rather than the irradiation power [14–18]. The plating temperature was controlled at 323 K. Higher power of microwave irradiation resulted in a shorter plating time, which indicated that the time of interaction between active sites and adsorbates was shortened. Then a higher power got a relatively lower Ni loading. Table 2 shows the binding energy of Ni and B in Ni–B/MgO(W) and Ni–B/MgO(EG) from XPS characterization. The binding energies of Ni and B in both catalysts are close to the Ni_2B compound.

Table 2
The results of XPS characterization for Ni–B/MgO(W) and Ni–B/MgO(EG)

Binding energy (eV)	Samples		Reference		
	Ni–B/MgO(EG)	Ni–B/MgO(W) [11]	B [23]	Ni_2B [24]	Ni [23]
B 1s	188.3	188.1	187.1	187.90	–
Ni $2p_{3/2}$	853.3	853.0	–	853.20	853.1

Fig. 2 presents the TEM micrographs of Ni–B/MgO prepared with different microwave irradiation power. When 60 W power is applied, the particle size of Ni–B particles in Ni–B/MgO(EG) is 45–50 nm (Fig. 2a). It is much smaller than that of Ni–B/MgO(W) (~85 nm, as shown in Fig. 2b). In comparison with Ni–B/MgO prepared by conventional heating, the particle size of Ni–B in Ni–B/MgO(W) increases sharply from ~40 nm to ~85 nm, while it changes somewhat in Ni–B/MgO(EG). This suggests that microwave irradiation affects the properties of Ni–B nanoparticles in aqueous plating solution more greatly than that in EG solution. The dielectric constant of water (ε, 293 K) is 58.8, while 8.85 for ethylenediamine and 26.33 for ethylene glycol [25,26]. For the sorption of oxide solids, the heat of adsorption of adsorbate with high ε was lower than that with low ε, and the adsorbate with low ε should be desorbed and the one with high ε was adsorbed in its place or desorbed to a lesser extent under conventional heating [15,17]. In the electroless plating solution, the nickel ions were stabilized by en due to the formation of $[Ni(en)_n(H_2O)_{6-2n}]^{2+}$ complex rather than $[Ni(H_2O)_6]^{2+}$ complex [19]. As the en/Ni molar ratio was 4, the nickel ions in plating solution were present in $[Ni(en)_3]^{2+}$ mostly and some $[Ni(en)_2(H_2O)_2]^{2+}$ [27]. The interaction between ethylenediamine and nickel ions was much stronger than that between water and nickel ions. Therefore, when the electroless plating was activated by silver, the resulting Ni–B clusters were mostly covered by ethylenediamine. The deposition of Ni–B clusters on support was depended on the sorption of ethylenediamine over supports. The adsorption of en was prior to water when conventional heating was applied. Then, the distribution of Ni–B was determined by the sorption of en on MgO, and the dispersion of Ni–B was homogeneous. When microwave irradiation was applied, the interaction between water and MgO was strengthened, and the sites for en adsorption became fewer, resulting in fewer sites for Ni–B deposition. Then the particle size of Ni–B particles grew to larger with a continuous deposition of Ni–B clusters on fewer sites. In contrast, the dielectric constant of ethylenediamine and ethylene glycol was closer, and the particle size of Ni–B changed much less (Figs. 1b and 2a).

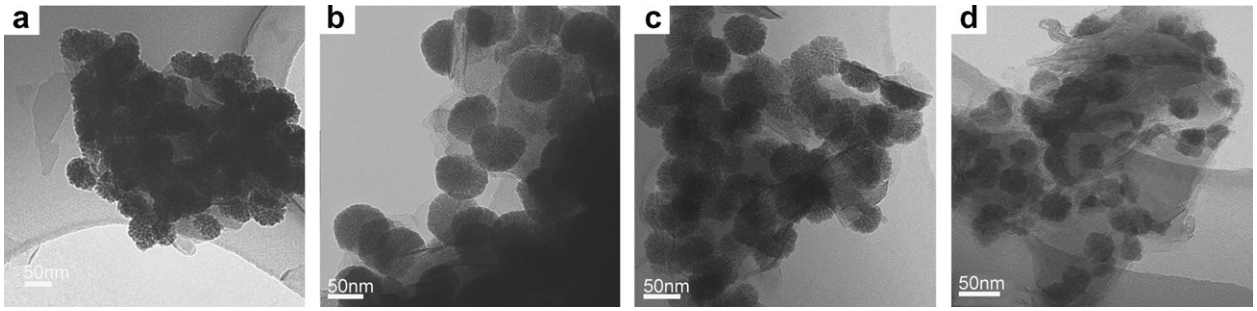

Fig. 2. TEM micrographs of supported samples prepared with different microwave irradiation powers. (a) Ni–B/MgO(EG) with 60 W; (b) Ni–B/MgO(W) with 60 W; (c) Ni–B/MgO(W) with 120 W and (d) Ni–B/MgO(W) with 180 W.

Fig. 2 shows that microwave irradiation has a significant effect on the particle size of Ni–B in Ni–B/MgO(W). When the microwave irradiation power is increased from 60 W to 180 W, the particle size of Ni–B in Ni–B/MgO(EG) is still held at 45–50 nm, while the particles size in Ni–B/MgO(W) decreases from ~85 nm to ~45 nm. The plating temperature was controlled at 323 K. A higher irradiation power applied leaded to a shorter irradiation time, such as 27 min for 60 W, 2.1 min for 120 W, and less than 1 min for 180 W. As the interaction between supports and adsorbates were strengthened with microwave irradiation time [14–18], the competitive adsorption of water and en was weakened with increasing microwave irradiation power. This could be explained by the XRD pattern of Ni–B/MgO(W) (Fig. 3). Although a broad peak around $2\theta = 45°$ due to amorphous Ni–B is not found in Ni–B/MgO(W) (Fig. 3a–d), the peaks ascribed to crystalline Ni are observed in the catalyst with crystallization treatment (Fig. 3e). This shows that the amorphous Ni–B particles are homogeneously dispersed over MgO and its low intensity of diffraction is beyond the detection limit of XRD. The MgO could convert into $Mg(OH)_2$ in the basic solution [28], and microwave irradiation promotes such conversion. As shown in Fig. 3, the amount of $Mg(OH)_2$ increases with decreasing microwave irradiation power. It means that more $Mg(OH)_2$ is formed with microwave irradiation time.

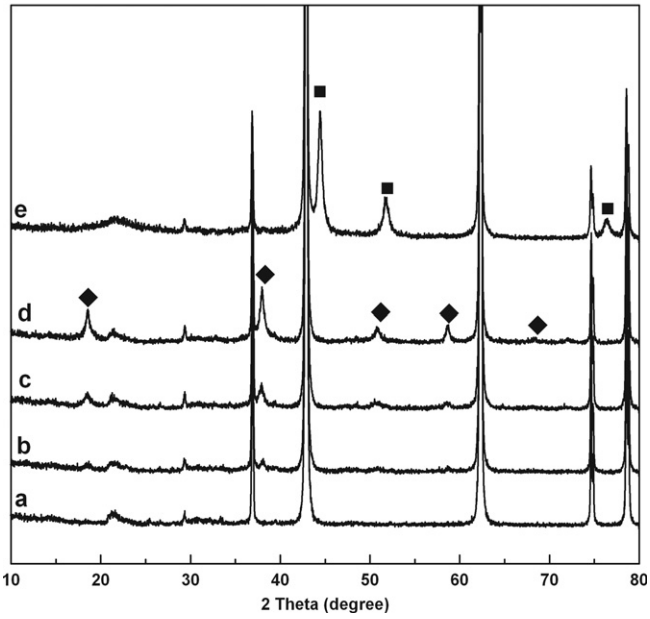

Fig. 3. XRD patterns of Ni–B/MgO(W) prepared under microwave irradiation with (a) 0 W power; (b) 180 W power; (c) 120 W power; (d) 60 W power; and (e) crystallized Ni–B/MgO(W) from (a). Solid diamonds, $Mg(OH)_2$ species; and solid squares, crystalline Ni species. The crystallization was carried out under a 40 ml/min argon flow at 723 K for 1 h.

3.2. Catalytic activities of supported Ni–B catalysts

The catalytic hydrogenation of organic derivatives containing a carbonyl group, is an important reaction for the preparation of intermediates in the fine chemicals and pharmaceutical industries [29]. The hydrogenation of acetophenone is particularly important because of the extensive industrial application of its possible reaction products: phenyl 1-ethanol (PE) and cyclohexyl 1-ethanol (CHE) (Scheme 1) [30–32]. The selectivity of PE and CHE depends on the electronic properties of catalyst, in which active metals rich in electrons prefer to adsorb C=O groups rather than aromatic rings, resulting in a higher PE selectivity [30–32]. Moreover, further hydrogenolysis of PE to styrene occurs, leading to the formation of ethylbenzene (EB) in the next hydrogenation, with increasing partial pressures of hydrogen or hydrogenation time. Thus, the hydrogenation of AP should be carried out at a lower hydrogen pressure in a short time.

Table 3 shows that the major hydrogenation product is PE rather than CHE on Ni–B/MgO catalyst from the results of product distribution. The selectivity of CHE on Ni–B/MgO(W) is higher than that on Ni–B/MgO(EG). For amorphous Ni–B catalyst, the Ni atoms accepted electrons from B, resulting in a high PE selectivity [33,34]. Table 1 indicates that the B content of Ni–B particles in Ni–G/MgO(EG) is higher. The Ni–B/MgO(EG) shows a higher binding energy of B 1s than Ni–B/MgO(W) (Table 2). These suggest that the more electrons are transferred from B atoms to Ni atoms in Ni–B/MgO(EG). The enrichment of electrons around active Ni sites in Ni–B/MgO(EG) restrains the absorption of aromatic rings, which prevents the formation of CHE.

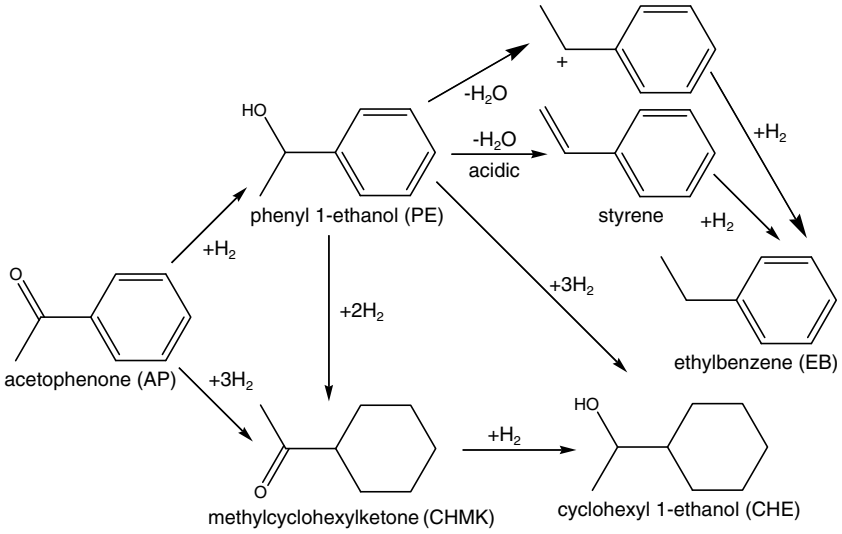

Scheme 1. Reaction scheme of acetophenone hydrogenation.

Table 3
The catalytic properties of Ni–B/MgO samples

Sample	Power of microwave (W)	Conversion (%)	Product distribution (%, selectivity)		
			PE	CHE	EB
Ni–B/MgO(W)	0	87.5	87.6	4.1	6.3
Ni–B/MgO(W)	180	73.2	89.4	3.7	4.4
Ni–B/MgO(W)	120	41.2	93.5	3.2	2.4
Ni–B/MgO(W)	60	21.7	95.4	3.2	0.7
Ni–B/MgO(EG)	0	82.5	94.7	1.3	3.5
Ni–B/MgO(EG)	180	83.4	94.6	1.2	3.5
Ni–B/MgO(EG)	120	87.3	94.8	1.2	3.2
Ni–B/MgO(EG)	60	93.2	95.1	0.9	3.0

For the formation of EB, it is gotten by two routes from AP as shown in Scheme 1: hydrogenolysis of PE to styrene and to carbenium ions. As the hydrogenolysis of PE to styrene is catalyzed by the acidic site of catalyst, the selectivity of EB decreases with increasing the content of $Mg(OH)_2$ on Ni–B/MgO(W) catalysts prepared under microwave irradiation (Fig. 3 and Table 3). The conversion of AP over Ni–B/MgO(W) decreases with decreasing microwave irradiation power. It is ascribed to the ascending particle size of Ni–B (Fig. 2). Table 3 shows that the selectivity of PE on Ni–B/MgO(W) is similar with that of Ni–B/MgO(EG) catalyst after 1 h hydrogenation. However, the selectivity decreases sharply to 12.3% with prolonging hydrogenation time to 4 h, while 55.3% selectivity is presented in Ni–B/MgO(EG) catalyst. This should be explained by the different electronic properties of catalyst. In summary, the supported Ni–B/MgO(EG) shows a better selectivity of PE. As the particles size of Ni–B in Ni–B/MgO(EG) is stable with microwave irradiation power, a higher conversion of AP on Ni–B/MgO(EG) shown in Table 3 should be due to the increase of nickel loading and boron content (Table 1). Li et al. found that the boron content of Ni–B particles affected the catalytic activity greatly [35]. The coordination number of Ni decreased with increasing boron content, showing that Ni active sites became more highly unsaturated. Such highly unsaturated Ni active sites promoted the chemisorptions of the reactants and, in turn, increased the hydrogenation activity. Here, the hydrogenation results show that the Ni–B/MgO(EG) is a suitable for AP hydrogenation, and its catalytic properties are promoted by microwave irradiation.

The following work is focused on studying the microwave irradiation conditions for Ni–B/MgO(EG) preparation. When the microwave irradiation powder is the same, different plating temperature requires different irradiation time. In this paper, the power of microwave irradiation was holed at 60 W, and the plating temperature was optimized. Table 4 shows the relations between plating temperature and the nickel loading and composition of Ni–B particles. The nickel loading and nickel content of Ni–B particles increase with microwave irradiation time and temperature. To study which factor is preferable for changing nickel loading and content, Ni–B/MgO (EG) are prepared with different irradiation time at 328 K (Table 5). After microwave irradiation (less than 31 min), the plating is carried out by conventional heating. Table 5 shows that the nickel loading increases with microwave irradiation time, while the nickel content in Ni–B particles

Table 4
The compositions of Ni–B/MgO(EG) samples prepared at different microwave irradiation temperature

Temperature (K)	Plating time (min)	Load of Ni (wt%)	Compositions (at%)
313	21	7.5	$Ni_{60.2}B_{39.8}$
318	24	8.3	$Ni_{61.4}B_{38.6}$
323	29	11.2	$Ni_{61.8}B_{38.2}$
328	31	11.6	$Ni_{63.8}B_{36.2}$
333	36	12.1	$Ni_{66.2}B_{33.8}$

Table 5
The compositions of Ni–B/MgO(EG) samples prepared with different microwave irradiation time at 328 K

Plating time (min)	Load of Ni (wt%)	Compositions (at%)
5	10.7	$Ni_{65.2}B_{34.8}$
10	10.7	$Ni_{64.4}B_{35.6}$
15	10.9	$Ni_{66.1}B_{33.9}$
20	11.3	$Ni_{62.8}B_{37.2}$
25	11.5	$Ni_{63.2}B_{36.8}$

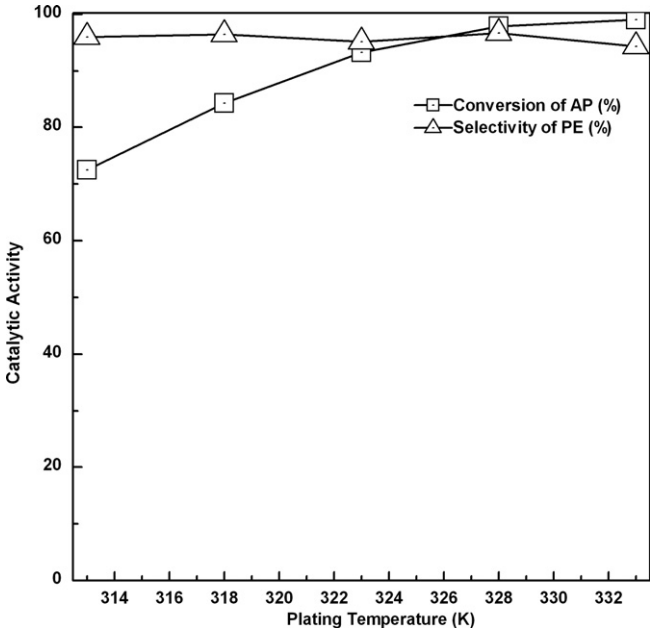

Fig. 4. Relations of plating temperature and the catalytic property of Ni–B/MgO(EG) catalyst.

decreases somewhat. Thus, the increase of nickel content in Table 4 should be ascribed to the change of borohydride oxidation or hydrolysis with plating temperature. Moreover, because of the deposited materials, Ag, Ni, and Ni–B are electronic conductors, the change of compositions may also be related with the influence of microwave irradiation on these electronic conductors. Fig. 4 shows the catalytic properties of Ni–B/MgO(EG) prepared at different microwave irradiation temperature. It suggests that the best preparation temperature under microwave irradiation is 328 K.

4. Conclusion

Supported Ni–B catalysts were synthesized by a silver-catalyzed electroless plating method in water bath and EG bath under microwave irradiation. The results showed that the nickel loading on Ni–B/MgO catalyst was promoted by the microwave irradiation. The increment of nickel loading resulted in growing particle size of Ni–B particles in Ni–B/MgO(W). On the other hand, the particle size of Ni–B particle in Ni–B/MgO(EG) catalyst changed somewhat under microwave irradiation. The hydrogenation results showed that the supported Ni–B catalysts exhibited excellent PE selectivity in the AP hydrogenation, and the Ni–B/MgO(EG) showed better catalytic activity and selectivity. The catalytic properties of Ni–B/MgO(EG) could be promoted by increasing microwave irradiation temperature and time.

Acknowledgements

The authors thank for the financial support of the National Natural Science Foundation of China (Grants 20403009), the Key Project of Chinese Ministry of Education (No. 105045).

References

[1] P. Schwarzkopf, R. Kieffer, W. Leszynski, F. Benesovsky, Refractory Hard Metals: Borides, Carbides, Nitrides, and Silicides, The Macmillan Company, New York, 1953.
[2] B. Ganem, J.O. Osby, Chem. Rev. 86 (1986) 763.
[3] H.C. Brown, C.A. Brown, J. Am. Chem. Soc. 85 (1963) 1005.
[4] Z.J. Wu, W. Li, M.H. Zhang, K.Y. Tao, Front. Chem. Eng. China 1 (2007) 87.
[5] E.Z. Min, C.Y. Li (Eds.), Base of Science and Engineering of Green Petrochemical Technology, Chinese Petrochem Press, Beijing, 2002.
[6] X.Y. Chen, W.L. Yang, S. Wang, M.H. Qiao, S.R. Yan, K.N. Fan, H.Y. He, New J. Chem. 29 (2005) 266.
[7] Z.J. Wu, M.H. Zhang, S.H. Ge, Z.L. Zhang, W. Li, K.Y. Tao, J. Mater. Chem. 15 (2005) 4928.
[8] S.H. Ge, Z.J. Wu, M.H. Zhang, W. Li, K.Y. Tao, Ind. Eng. Chem. Res. 45 (2006) 2229.
[9] S.H. Ge, Z.J. Wu, M.H. Zhang, W. Li, K.Y. Tao, Chin. J. Catal. 27 (2006) 277.
[10] Z.J. Wu, S.H. Ge, M.H. Zhang, W. Li, K.Y. Tao, J. Phys. Chem. C 111 (2007) 8587.
[11] Z.J. Wu, M.H. Zhang, W. Li, K.Y. Tao, J. Mol. Catal. A 273 (2007) 27.
[12] D.M.P. Mingos, Chem. Ind. (1994) 596.
[13] D.E. Clark, W.H. Sutton, Annu. Rev. Mater. Sci. 26 (1996) 299.
[14] M.D. Turner, R.L. Laurence, W.C. Conner, K.S. Yngvesson, AICHE 46 (2000) 758.
[15] M.D. Turner, R.L. Laurence, K.S. Yngvesson, W.C. Conner, Catal. Lett. 71 (2001) 133.
[16] W.C. Conner, G. Tompsett, J. Phys. Chem. B 108 (2004) 13913.
[17] S.J. Vallee, W.C. Conner, J. Phys. Chem. B 110 (2006) 15459.
[18] G.A. Tompsett, W.C. Conner, K.S. Yngvesson, Chem. Phys. Chem. 7 (2006) 296.
[19] G.O. Mallory, J.B. Hajdu, Electroless Plating: Fundamentals and Applications, American Electroplaters and Surface Finishers Society, Orlando, FL, 1990.
[20] W. Riedel, Electroless Nickel Plating, ASM International, Finishing Publications, 1991.
[21] X. Yin, L. Hong, B.H. Chen, J. Phys. Chem. B 108 (2004) 10919.
[22] I. Ohno, O. Wakabayashi, S. Haruyama, J. Electrochem. Soc. 132 (1985) 2323.
[23] H. Li, H.X. Li, W.L. Dai, W.J. Wang, Z.G. Fang, J.F. Deng, Appl. Surf. Sci. 152 (1999) 25.
[24] J. Legrand, A. Taleb, S. Gota, M.J. Guittet, C. Petit, Langmuir 18 (2002) 4131.
[25] C. Reichardt, Solvents and Solvent Effects in Organic. Chemistry, VCH, Weinheim, 1988.
[26] N.L. Cheng, Handbook of Solvents, Chemical Industry Press, Beijing, China, 1999.
[27] K.Q. Sun, E. Marceau, M. Che, Phys. Chem. Chem. Phys. 8 (2006) 1731.

[28] K. Refson, R.A. Wogelius, D.G. Fraser, Phys. Rev. B 52 (1995) 10823.
[29] M. Casagrande, L. Storaro, A. Talon, M. Lenarda, R. Frattini, E. Rodríguez-Castellón, P. Maireles-Torres, J. Mol. Catal. A 188 (2002) 133.
[30] T. Koscielski, J.M. Bonnier, J.P. Damon, J. Masson, Appl. Catal. 49 (1989) 91.
[31] J. Masson, S. Vidal, P. Cividino, P. Fouilloux, J. Court, Appl. Catal. 99 (1993) 147.
[32] S.D. Lin, D.K. Sanders, M.A. Vannice, J. Catal. 147 (1994) 370.
[33] Y.Z. Wang, M.H. Qiao, H.R. Hu, S.R. Yan, W.J. Wang, K.N. Fan, Acta Chim. Sinica 62 (2004) 1349.
[34] C.Q. Xu, D.J. Zhu, G.Q. Li, J. Mol. Catal. (Chinese) 18 (2004) 281.
[35] H.X. Li, H. Li, W.L. Dai, M.H. Qiao, Appl. Catal. A 238 (2003) 119.